Solidification of a water-saturated granular medium and solute migration

Justine QUENTIN [1] [2]

Tuteurs : Axel Huerre[3] [4], Thomas SEON[5]

Université Paris Cité [1]

Université Franco-Italienne [2]

[3]Laboratory Matière et Systèmes Complexes (MSC), Université Paris Cité

[4]Institut Jean le Rond d'Alembert, Sorbonne Université

[5]IRL Institut Franco-Argentin de Dynamique des Fluides pour l'Environnement (IFADyFE), University of Buenos Aires

Contents

Key words : Solute migration, water-saturated granular medium, solidification, modeling

Many thanks to Thomas Séon, Axel Huerre, Veronica D'angelo, Veronica Raspa Krishan Bumma and Lila Séguy for supervising me and for their precious advices.

1 Introduction

1.1 A new CNRS laboratory

The study of this subject through my internship was mainly carried out at the new International Research Laboratory (IRL), Institut Franco-Argentin de Dynamique des Fluides pour l'Environnement (IFADyFE) in Buenos Aires, Argentina. This institut is the fruit of over 40 years of scientific collaboration between French and Argentine researchers in fluid mechanics. Opened in January 2024, it is a fluid mechanics research centre with environmental applications at the heart of today's concerns. This INSIS-CNRS IRL is a joint project with CONICET and the University of Buenos Aires (UBA) and will help to strengthen this international collaboration. Among others, the laboratory is interested in a wide variety of natural phenomena involving the movement of fluids: in oceans, atmosphere, rivers, glaciers, volcanoes, permafrost, groundwater, etc. These studies are essential for understanding the Earth's climate system and for predicting the effects of natural disasters, which are multiplying and intensifying as a result of ongoing global warming.

1.2 Subject under study : the permafrost

The permafrost is a subject of physics of soils, it refers to ground a permanently frozen on top of which rests an different layer of soil which is frozen or thawed in part depending on the season. Permafrost exists at high latitudes and altitudes and covers 20% of the Earth's surface (see Fig.1). The surface layer is called "active" layer (see Fig.2) and is sensitive to changes in temperature, freezing in winter and thawing in summer. The movement of a solidification front in the ground modifies its structure and can lead to underground flows that alter its stability and, in particular, cause specific macroscopic shapes to appear on the surface. Climate change is causing permafrost to melt, lead to specific macroscopic events that are that appear on landscapes and ecosystems (see Fig.3). These events are becoming increasingly frequent and are having an important impact on infrastructure in these areas.

Moreover, it is important to notice that since the laboratory is new, there were no equipment when I begun my internship. I had to find alternative solutions and improvise with the resources available, as well as taking the necessary steps to obtain the necessary equipment and carry out the experiments successfully. What's more, the subjects of study is also new and my experiment was still to be built up.

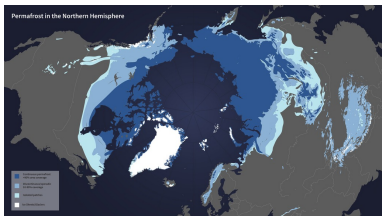

Figure 1: Main regions of the Earth underlained by permafrost [10]

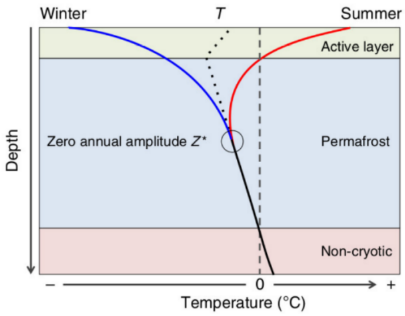

Figure 2: Extreme seasonal temperature profile as a function of depth in periglacial ground [4]

Figure 3: Example of a patterned ground on the surface of a periglacial ground from [8]

Studying the active layer is interesting to understand how heat transfers and phase changes change the structure of soil. Since this layer is composed of a complex frozen mixture of soil, rock, water and organic matter, the heat transfers modify the quantity of water in this medium and make the overall structure of the soil unstable, in particular by changing the distribution of the granular medium. Thus, it is important to study, through fluid dynamics, this phenomenon and the impact of frost stress on soil structure to understanding the solidification processes and interactions between soil components.

2 The theoretical models

The first subject of interest will be the study of the solidification front dynamic in a porous media which can model the soil behavior. Thus, we are going to concentrate on characterising the speed of the growth of this solidification front in a 2-phase medium subject to freezing. We will deal with the Stefan problem (see section 2.1), a fundamental concept in the study of phase change phenomena, offering insights into how materials undergo a phase transition in response to thermal conditions.

The second subject of interest will be to study the emergence of instabilities on the solidification front during its growth, and the appearances of channels of liquid in the medium. We will deal with the concept of Mullins-Sekerka instabilities (see section 2.2) wich represent a fundamental aspect of solidification dynamics, influencing the microstructure and properties of solidified materials.

By these two studies we try to understand the influence of solidification on the structure of the soil and to observe the relative movements between the grains, the ice, the water and polutants inside the water.

2.1 Heat transfert and Stefan problem

To study phase transitions in matter, we deal with the Stefan problem [11] which caracterises the freezing front propagation dynamics for a one-dimensional liquid system. It is a particular kind of boundary value problem, for a system of partial differential equations, in which the boundary between two phases can move with time as shown on Fig.4. We will derive below the most general case of a 2-phase system of a solid phase in contact with a liquid one and lying on a cold substrate.

In our case, we are dealing with a layer of ice resting between a semi-infinite solid substrate and a semi-infinite water, a case on which a variant of the Stefan problem exists [14][12] and our goal here is to find its solution.

It is important to notice that $C_p\Delta T$ is small compared with the latent heat L, so the energy needed to bring the water to 0 degrees is neglected. It is therefore assumed that the water is already at 0 degrees, so there is no flow in the water. So by considering only the 1-D heat equations in the substrate and in the ice :

$$(\rho C_p)_k \frac{\partial T}{\partial t} = \lambda_k \frac{\partial^2 T}{\partial z^2} \tag{1}$$

with the subscript k being s for the substrate at the bottom ($z \leq 0$), i for the solid ice ($z \leq h(t)$), and l for the liquid water ($h(t) \leq z$). The parameters ρ, C_p and λ are respectively the density, heat capacity and heat conductivity for our material. Now we deal with the different temperatures at the boundaries of the phases. The discontinuity of heat fluxes due to latent heat at the ice-water interface is expressed by the Stefan condition. In our case, here we are omiting the flux in water and get :

$$\rho_s \mathcal{L} \frac{dh}{dt} = \lambda_s \frac{\partial T}{\partial z}(h^-, t) \tag{2}$$

$$\lambda_s \frac{\partial T}{\partial z}(0^-, t) = \lambda_i \frac{\partial T}{\partial z}(0^-, t) \tag{3}$$

$$\lambda_i \frac{\partial T}{\partial z}(h(t)^-, t) = \rho_i \mathcal{L} \frac{dh}{dt} \tag{4}$$

Test $D_{eff,solide} \approx 4.5 \cdot D_{eff,ice}$ $D_{eff} = 2 \cdot St \cdot D$

with $\mathcal{L}$ the latent heat of solidification of the water.

Similarity analysis shows that this diffusive problem exhibits a self-similar structure. In this case, the solidification front location follows also a square-root in time law, showing the diffusive property of the dynamics. Consequently, the growth of the freezing layer follows the classical diffusive dynamics : $h(t) = \sqrt{D_{\text{eff}} \cdot t}$. The coefficient D_{eff} is the effective diffusion coefficient that depends on the temperatures at the boundaries and the thermal properties of the ice [6]. Our goal is to compute D_{eff} with unit coefficient : square metre per second m^2/s.

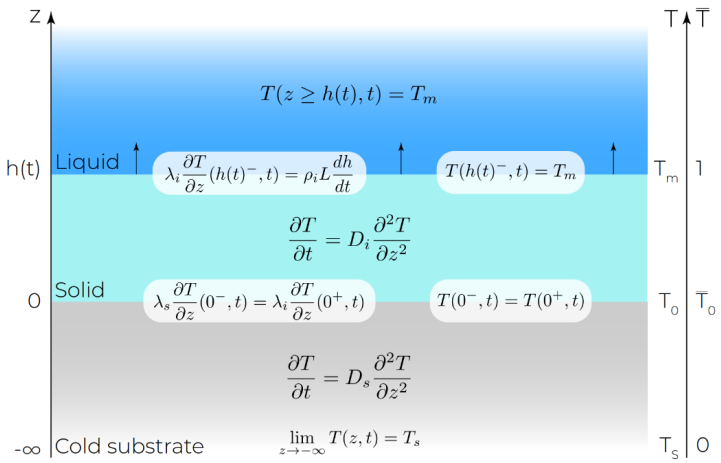

Figure 4: Summary of the model hypotheses: A finite layer of solid lies between the semi-infinite melt ($z > h(t)$) and the semi-infinite substrate ($z < 0$). The temperature of the whole melt is set constant at the melting point ($T = T_m$), while the temperature of the substrate tends to T_S when $z \to -\infty$. The temperature in the solid phases is given by a set of two heat equations, with a specific diffusion coefficient D_k for each phase, coupled by the temperature and heat flux continuity at $z = 0$. At the solidification front ($z = h(t)$), the Stefan condition imposes the downward thermal flux to be equal to the latent heat liberated by the freezing (figure from [13]).

Introducing the self-similar variable in the set of equations 1, 4 which are also shown in Fig. 4, we obtain the following solutions for the temperature field:

$$T(z,t) = T_0 + (T_0 - T_s) \cdot \mathrm{Erf}\left(\frac{z}{2\sqrt{D_s t}}\right) \quad \text{for} \quad z \leq 0 \tag{5}$$

and

$$T(z,t) = T_0 + \frac{e_s}{e_i}(T_0 - T_s) \cdot \mathrm{Erf}\left(\frac{z}{2\sqrt{D_i t}}\right) \quad \text{for} \quad 0 \leq z \leq h(t) \tag{6}$$

where $e_{s,i} = \sqrt{\lambda_{s,i}\rho_{s,i}C_{p,s,i}}$ are the effusivities [1] of the substrate and the solid, and T_0 the contact temperature at the solid-substrate interface, a constant in time in this self-similar framework. T_0 is an integration constant to be determined by the boundary conditions. Then, by imposing the Stefan condition at z = h(t), we obtain the following transcendental equation [13]:

$$St = \sqrt{\frac{\pi\beta}{2}} \cdot \exp\left(\frac{\beta}{4}\right) \cdot \left(\frac{e_i}{e_s} + \mathrm{Erf}\left(\frac{\sqrt{\beta}}{2}\right)\right) \tag{7}$$

with β defined as $\beta = \frac{D_{eff}}{D_i}$ and St the Stefan number defined as $St = \frac{C_{pi}(T_m - T_s)}{L}$. This last equation 7 has to be solved numerically.

2.1.1 Quasi-static resolution of Stefan problem

This problem can be solved in the quasi-static approximation. Our solid phase is assumed to rest on a substrate at temperature T_s constant and the liquid phase is assumed to have a uniform 0°C temperature. The Stefan condition is then the same as eq.4 at the interface. Then, eq.1 can be rewritten as :

$$\frac{\partial T}{\partial t} = D_i \frac{\partial^2 T}{\partial z^2} \tag{8}$$

[1] The effusivity of a material is the physical quantity that witnesses both its heat capacity and its ability to diffuse it.

In the quasi-static approximation, the temperature in the media does not depends on the position so we get :

$$\frac{\partial T}{\partial t} = 0 \tag{9}$$

$$\frac{\partial^2 T}{\partial z^2} = 0 \tag{10}$$

By solving this second derivative equation we get :

$$\frac{\partial T}{\partial z} = K_1 \rightarrow T = K_1 \cdot z + K_2 \tag{11}$$

By considering the boundary conditions and considering a substrate at -10°C :

$$T = \frac{\Delta T}{h} \cdot z - 10 \tag{12}$$

Then eq.4 can be expressed in the quasi statique approximation as :

$$\rho_s \mathcal{L} \frac{dh}{dt} = \lambda_s \frac{\Delta T}{h} \rightarrow \frac{\rho_s \mathcal{L}}{\lambda_s \Delta T} h dh = dt \tag{13}$$

Since $\Delta T/h \propto \frac{dh}{dt}$, the dynamic propagation of the front over time is inversely proportional to the height of the front, hence the square-root growth that will follow later. After integration of eq.13 we get :

$$\frac{\mathcal{L}}{C_p \cdot \Delta T \cdot D} \frac{h^2}{2} = t \tag{14}$$

with the diffusion coefficient :

$$D = \frac{\lambda_s}{\rho_s C_p} \tag{15}$$

Then we get the Stefan number :

$$St = \frac{(C_p * \Delta T)}{\mathcal{L}} \tag{16}$$

Finally, we can solve eq.14 and express the height of the front as the square root of the Stefan number St, the diffusion coefficient for ice D_i and the time t :

$$h(t) = \sqrt{2 \cdot St \cdot D_i \cdot t} \tag{17}$$

2.2 Mullins-Sekerka instabilities

The Stefan problem describes the propagation of a planar front. For certain conditions, this front is unstable and instabilities can develop. The most common one is called the Mullins-Sekerka instabilities, named after the mathematicians that solved the problem historically.

During the solidification of a liquid, the interface is generally subject to various forces and influences of different parameters, such as the temperature gradient and the diffusion of impurities or chemical compounds. Mullins-Sekerka instabilities describe how small perturbations on this interface can grow and lead to irregular shapes or pattern-forming process in solidification [3].

In our experiment, which we will describe in detail below in sec.3, we freeze water mixed with a coloured tracer, fluorecein with his local concentration $C(z,t)$ depending on position and time.As the solidification front passes through the porous medium, the freezing of water will form a pure ice. The pollutant is thus expelled from the solid to the layer ahead of the freezing front, modifing the local concentration $C(z,t)$ of fluorecein.

In the Mullins-Sekerka instabilities for a flat interface between a liquid phase and a solid phase, the equation for the temperature [7] in the media as a function of concentration $C(z,t)$ simplified reads :

$$T(z,t) = T_m + m * C_{fluo} \tag{18}$$

where:

- $T(z,t)$ is the temperature at position z and time t.
- T_m is the melting temperature of the pure substance.
- m is a constante.
- C_{fluo} is the concentration at position z and time t of fluorecein.

This eq.18 shows that the higher the concentration of fluorescence in water, the lower its melting temperature (liquid form at lower temperature) and therefore the front will propagate more slowly at this point [9]. This relation between local temperature and concentration leads to destabilisations of the front that we develope in sec.4.2.2. This phenomenon is analogous to that of brine discharge, where seawater freezes by expelling the salt it contains [15].

3 The experimental setup

The experiment consists of freezing a mix of ceramic grains immerged into water with fluorescein. It is contained in a cell placed on a cold substrate and cooled from below. We want to measure the dynamics of the rise of the ice front as well as the final structure of the column shown in Fig.6. The grains are Microblast Electrofused ceramic beads, the fluorescein is in the form of sodium salt. The rectangular cell is made of 3 plexiglas sides and a microscope slide for the front side, forming a cell of dimension : 2.57cm of width, 1.5 cm for the thickness and 5cm of height. The cell is equipped with a double-glazed as front screen shown in Fig.5 to prevent condensation forming on the glass, which would create a blurred layer on the glass that would hide the column of grains behind. This double glazing is made up of 2 microscope slides of 1mm thickness and spaced by a 0.5mm thick rubber electrical sheath. The double glazing and the cell are sealed with sealant. It is important to note that the formation of condensation on the glass was the major problem in this experimental set-up. The choice of double glazing was made after numerous tests were carried out to avoid this condensation (see 7.2 for more details).

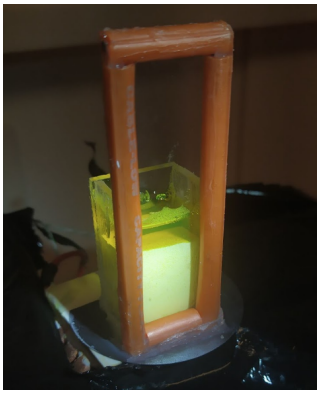

Figure 5: Final double glazing cell of 0.7 cm of thickness

The cold source is provided by a peltier device which is a thermoelectric module that is a stable cooling source. It is connected to a control software plugged to power supply. The peltier has a cold side that provides the desired temperature for the experiment and removes the heat from the opposite side. The heat released by the peltier is evacuated by a heat exchanger immersed in an ice bath as it is shown on Fig.6. To evacuate the heat and ensure that the temperature supplied by the peltier remains stable, the ice bath

should not be above 5 degrees Celsius.

Our approach will be to vary several parameters :

Parameters	**Values**
Ceramic grain size	125-250 μm and 250-425 μm
Peltier temperatures	-5°C, -10°C, -15°C
Fluorescein concentration in water	0.3 g/L, 0.6 g/L, 1.2 g/L, 2 g/L

Table 1: Summary of experimental parameters

The room temperature was 20°C. The fluorecein plays the role of a tracker since it appears yellow when the mix with the grains is liquid and orange when the mix is solid as we can see in the schematic cell of Fig.6.

Before each series of measurements, when the grains are placed in the cell, I carefully tamp the mixture to compact the grains in order to reduce the volume and increase the apparent density. This is done in order to obtain samples with a controlled and uniform compacity from one experiment to the next. By tamping the cell before each experiment, I aim to standardise the geometry of the samples, thereby minimising experimental variations due to differences in bulk density or grain arrangement.

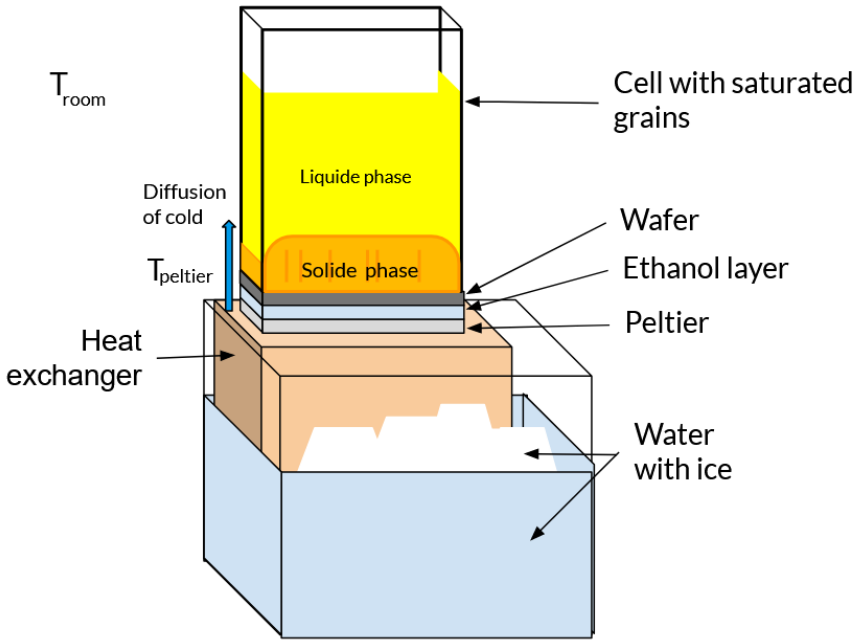

Figure 6: Scheme of the experimental setup

The method finally adopted is that of the 0.7 cm double-glazed cell combined with soap on the outer pane of the double-glazed cell and a brush to remove the frost excess when necessary. We use soap prevents fogging mainly by reducing the surface tension of the water and creating a uniform film that prevents condensation into small droplets. In addition, the ice/water tank was covered with plastic to prevent evaporation from the tank.

4 Experimental results

4.1 Height of the front

In the context of permafrost, a first study of a complex media made of foam, which are gas bubbles trapped in a liquid under solidification, was investigated in the group of research [2]. The dynamics of this structure can be compared to that of a mushy layer containing solid crystals surrounded by interstitial liquid [5]. In this previously cited article, the analysis of the solutions of the perturbative equations to determine stability leads to a theoretical model describing the instabilities and variations in the structure during solidification.

The study about foam [2] is proposing an analytical theory applied to the foam and led to a resolution of the Stefan equation allowing to caracterise the dynamics of the front in this case. We found a dynamic in the square root of time while taking into account the thermal parameters of the two media and the arrangement of the bubbles in the diffusion coefficient.

The next idea is to see if this 'continuous medium' approach is valid for granular materials. We now need to solve this problem by not just having a liquid medium but rather a medium that mixes grains and water. This granular medium gives us a microscopic structure and interaction mechanisms closer to those of soil. Thus, it was decided to study ceramic grains of various sizes immersed in water and characterise their behavior under controled temperature of freezing.

The image sequence of Fig.12 shows the propagation of the solidification front for our experiment. We are measuring the solidification front growth in time for a fix substrate temperature, a chosen size range of grains and a concentration of fluorecein in water. The front position is measured every 20 second. Thus, we can see how the column of grains placed on the cold substrate reacts to solidification, on the Fig.12 below.

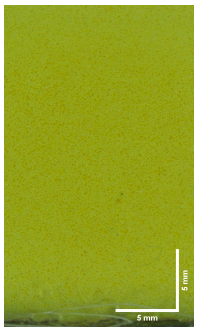

Figure 7: 0 sec

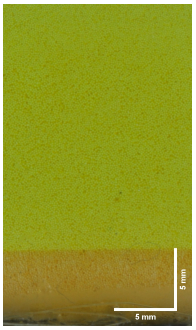

Figure 8: 100 sec

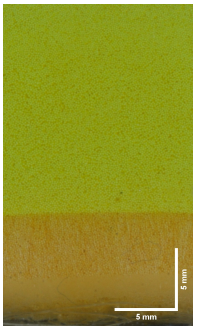

Figure 9: 200 sec

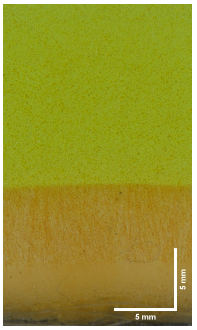

Figure 10: 300 sec

Figure 11: 400 sec

Figure 12: Exemple of front growth for grains of 120-180 μm at -15°C at with a concentration of 2 g/L of fluorecein

Thanks to the properties of fluorecein, the solidification front stands out and appears orange contrasting with the yellow liquid phase. We are using a local threshold method on the green channel of RGB images to localise the front[2] (see 4.2.1). We can see that the entirely liquid column at 0sec becomes increasingly orange as the solidification front progresses upwards. We expect to find a time-root behaviour as expressed in section 2.3.

[2]In fact, Orange is a combination of red and green, with the red component generally higher than that of green. The brightness difference between liquid and frozen foam gives an uncertainty for the measurement

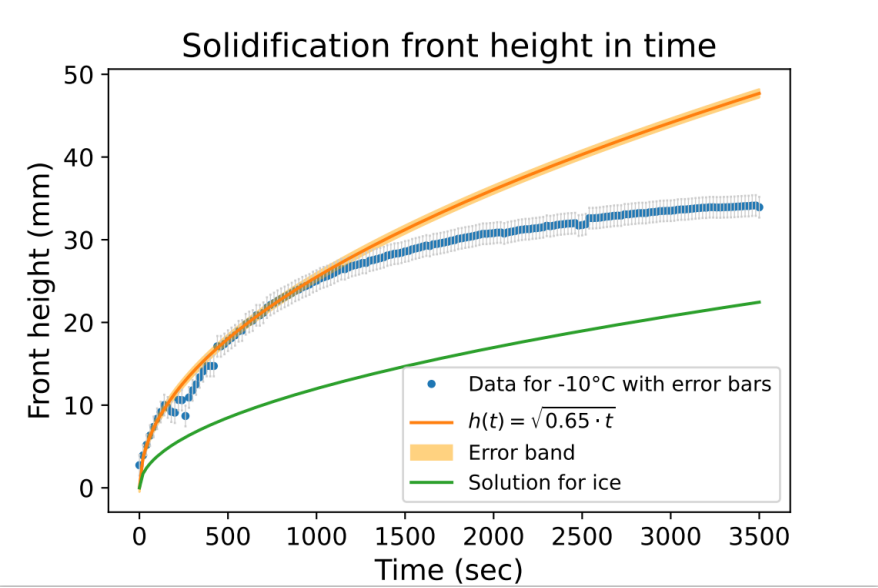

Figure 13: Growth of the freezing front for $T_s = -10°$C,R = 250-425 μm and concentration of fluorecein of $1.2 g/L$ and compared to the water growth of the freezing front (green line)

In Figure 13, we plot in blue the position of the ice front as a function of time and we plot in orange the curve $h(t) = \sqrt{0.65 \cdot t}$. We can see that the front grows has a square root behavior during the first 1000 secondes and then the dynamique is slowing and does not follows anymore a square root increase. We are expecting the front rise to follow a power law dynamic as a square root of time $h(t) \propto \sqrt{t}$.

The light-orange zone represents the uncertainty of the automated measurements. The green line is the result of the 1D model for pure water, and the green line is a 0.65 power-law fit of the experimental data. If the dynamic follows in fact the square root behavior, we expect in a log-log scale representation that the height of the front to have a first polynomial behavior.

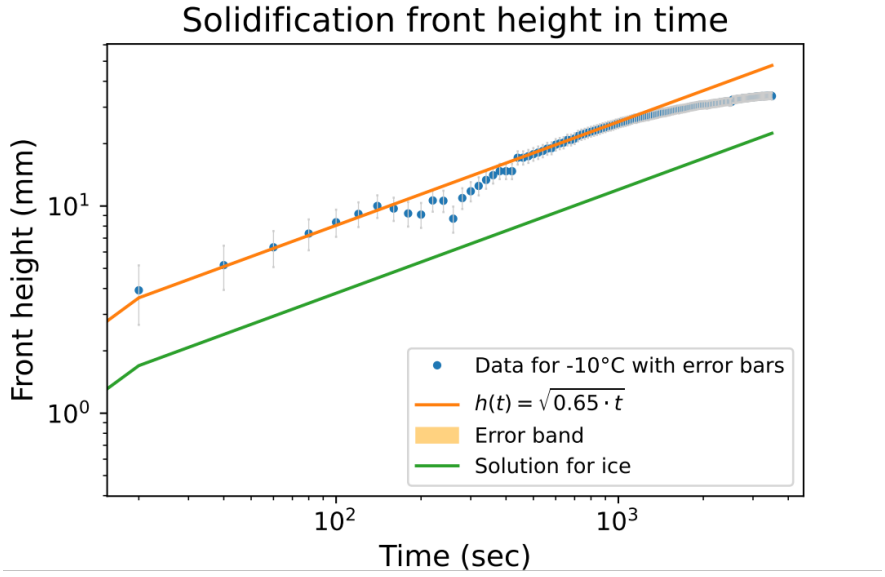

Figure 14: Growth of the freezing front for $T_s = -10°$, R = 250-425 μm and concentration of fluorecein of $1.2 g/L$ and compared to the water growth of the freezing front (green line) in logarithmi scale

We can see that our measurements follow a power law behavior as it can be approximated by a straight line in log-log representation (red line in Fig.14).

We can compare the dynamic of our front with the one of a simpler system with a front solidification growth that we can derive. The reference will be the quasistatic front growth of pure ice derived in section below. This ice dynamique is calculated at 0°C as follows :

The latent heat of fusion is given by:

$$L = 333\,\mathrm{kJ}\cdot\mathrm{kg}^{-1} \tag{19}$$

The specific heat capacity of ice is:

$$C_p = 2.06\,\mathrm{kJ}\cdot\mathrm{kg}^{-1}\cdot\mathrm{K}^{-1} \tag{20}$$

The thermal diffusion coefficient of ice is $D_i = 1.2$. The Stefan number associated is then :

$$\mathrm{St} = \frac{C_p \Delta T}{L} \tag{21}$$

Putting eq.21 back into eq.17 we get effective diffusion coefficient for $\Delta T = 10°\mathrm{C}$:

$$D_{\mathrm{eff},i} = 2 * St * D_i = 0.144\mathrm{m}^2/\mathrm{s} \tag{22}$$

Thus, the effective diffusion coefficient in our experiment $D_{\mathrm{eff,exp}}$ is much greater than that of ice since :

$$D_{\mathrm{eff},i} < D_{\mathrm{eff,exp}} \tag{23}$$

So our medium of immersed grains diffuses heat more quickly than pure ice. The difference in dynamics can be explained by the fact that ceramic grains have a diffusion coefficient $D = 1.95\mathrm{m}^2/\mathrm{s}$ [1] which is higher than the water one. This ifference can explain the faster front growth of mix of water and grains with respect to the growth of the pure ice of Fig.13 and Fig.14.

In the contrary and as a comparaison, in the study of the foam [2] it was shown that the system was less diffusive than the water. This would be explained by the fact that the air inside the foam reduces the capacity for heat exchange with the cold substrate.

4.2 Channels and instabilities

4.2.1 Image analysis

The analysis of solidification in the cell is carried out using a Nikon D800E camera with a 200mm zoom. A photo in RGB is captured every 20 seconds. To stop the presence of channels in the frozen zone, the image ImageJ is used for cropping and separation of the red, green and blue color channels, and after a contrast adjustment. The aim is to highlight the fluorescein channels for better identification by eyes. In the figure below Fig.19 we can see that extracting the blue channel is crucial to see well the fluorecein channels.

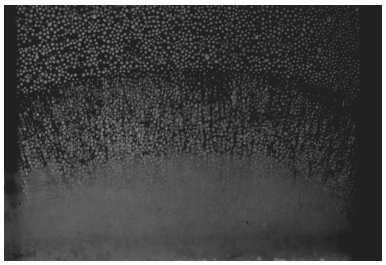

Figure 15: Blue channel on which we can see the fluorecein channels

Figure 16: Green channel without visible fluorecein channels

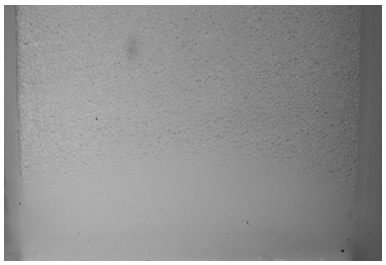

Figure 17: Red channel without visible fluorecein channels

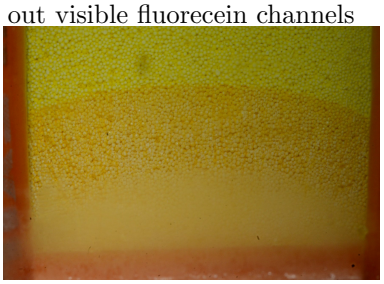

Figure 18: RGB image where you can already see a little the fluorecein channels

Figure 19: Example of splitting channel for a cell with grains of size 125-250 μm at -15°C for a fluo concentration of 2 g/L presenting fluorecein channels

When the colour channels of an image are extracted, each color channel (red, green and blue) shows the respective intensities of that colour in each pixel of the image. Orange has little or no blue component. The colours on a screen are created by combining different intensities of red (R), green (G) and blue (B). The colour orange is mainly composed of red and green, with little or no blue. So orange areas in an RGB image appear dark in the blue channel because there is little blue contribution.

All the experiments do not let to an appearance of fluorecein channels as we can see on the images below :

Figure 20: Blue channel

Figure 21: Green channel

Figure 22: Red channels

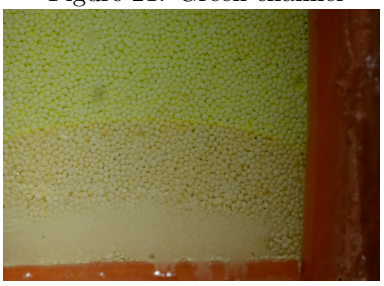

Figure 23: RGB image

Figure 24: Example of splitting channel for a cell with grains of size 125-250 μm at -15°C for a fluo concentration of 0.3 g/L not presenting fluorecein channels

We can see on the images above how look the bulk when there are no fluorecein channels.

4.2.2 Creation process of channels and phase diagram

As mentioned before, our experiment consists in freezing a cell placed on a peltier element, filled with ceramic grains of a single size, immersed in water and mixed with a dye (fluorescein powder suspended in water, colloidal mixture). This dye gives a yellow colour to the mixture and becomes more orange as it becomes more concentrated.

Ice expels impurities when it solidifies. So the solutes, in this case, the fluorescent particles present in the freezing water, are expelled from the forming ice to the liquid above it. The ceramic grains are too heavy to be expelled. Some of the fluorecein then concentrate in particular zones forming microscopic channels in the ice. We can suppose that these traces of the dynamics of solidification might be due to Mullins-Sekerka instabilities [3] (see sec.2.2). In the figures Fig.4.2.2,4.2.2 below, we can see the process of channel formation.

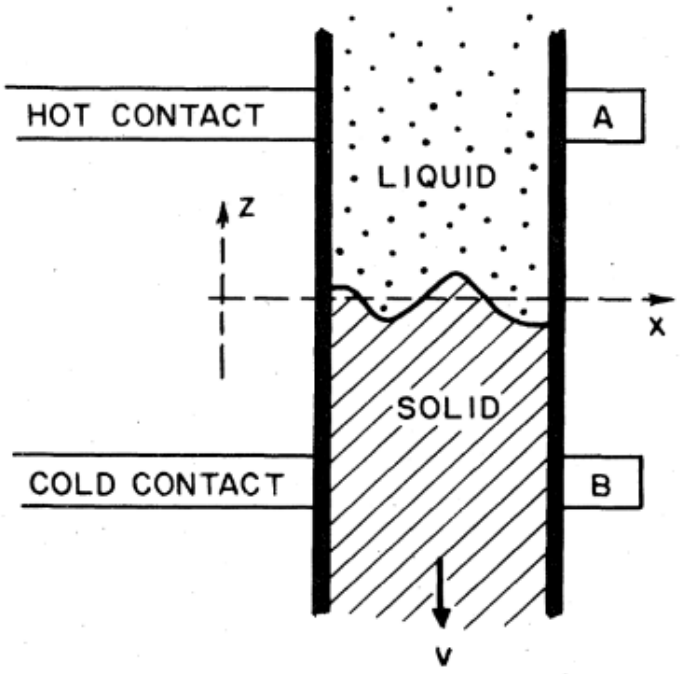

Figure 25: Schematic arrangement of a directional-solidification. experiment [9]

A zoom at the interface would give a better view of the the phenomenon involved. The figure below shows the origin of the channels and highlights their periodicity with a wave length λ.

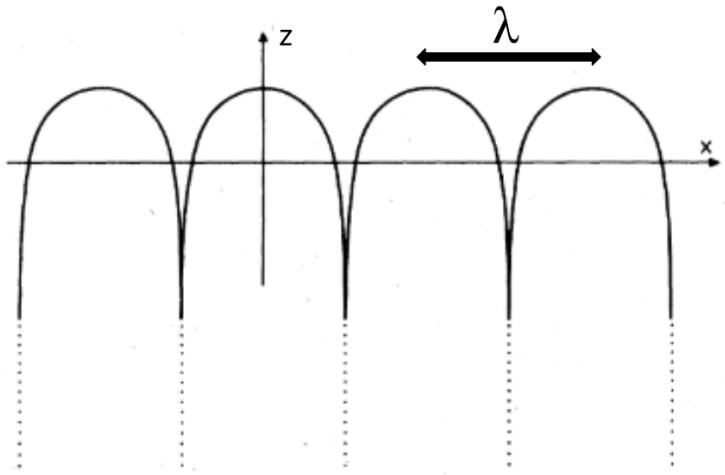

Figure 26: Cellular interface in directionally solidifying sample. The solidification front is moving in the positive-z (upward) direction and λ is the perturbation wave length [9]

The speed of the front can slow down enough at this point to be below the critical speed that causes the Mullins-Sekerka phenomenon. This irregularity will evolve into a well towards which the nearest particles will be conducted, further accentuating the attraction process. The solidification front continues to rise in the cell on either side of this well, which is over-concentrated in dye particles and becomes a channel as the ice advances around it. These channels of water over-concentrated in ice appear more orange than the surrounding mixture of grains and ice. So the inhomogeneity of colour is an indicator of the flow of pigment molecules in the channels. However, a slight increase in the concentration of water at a point on the front

will lead to irregularity and instability at the solid-liquid interface. We then have highly concentrated flows of water towards the solidification front. The increase in the melting point of liquid in the channels is what keeps them in the liquid phase. There is an equilibrium between the concentration and the local temperature in the channels and it no longer freezes, so the concentration will be directly given by the temperature.

Now let's if we look closer to the arrangement of the canals we can spot some periodic setting.

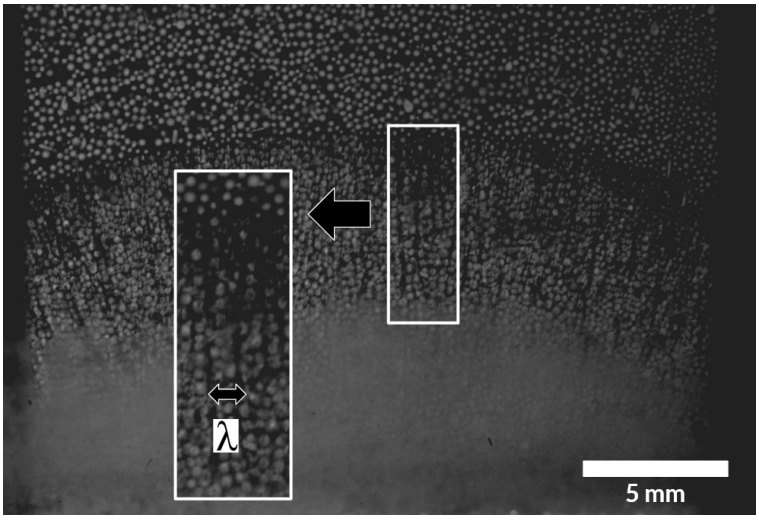

Figure 27: Image cell with grains of size 125-250 μm at -15°C for a fluo concentration of 2 g/L presenting fluorecein channels with a wave length λ

Looking at the distribution of the channels in the cell of Fig.4.2.2, we can guess that they seem to be distributed according to a certain periodicity. It would be interesting to take this analysis further and look for a characteristic wave length in the continuation of the study of solidification and compare it with the Mullins Sekerka one.

Experiments to see the presence of channels have been started before my internship by my research group. Under certain conditions of propagation speed of the front and size of the ceramic grains, we observe an expulsion with different behaviours. My contribution was to fill up a size range of grains by testing new sizes which had not been tested : 125-250 μm and 250-425 μm. To characterise the conditions of appearance the the fluorecein channels, we draw a phase diagramm of their presence depending on the bead range sizes and the concentration of fluorecein in the water. The measurements already done appear with a a solid black outline and mine appear with a dots outline on the phase diagram shown below.

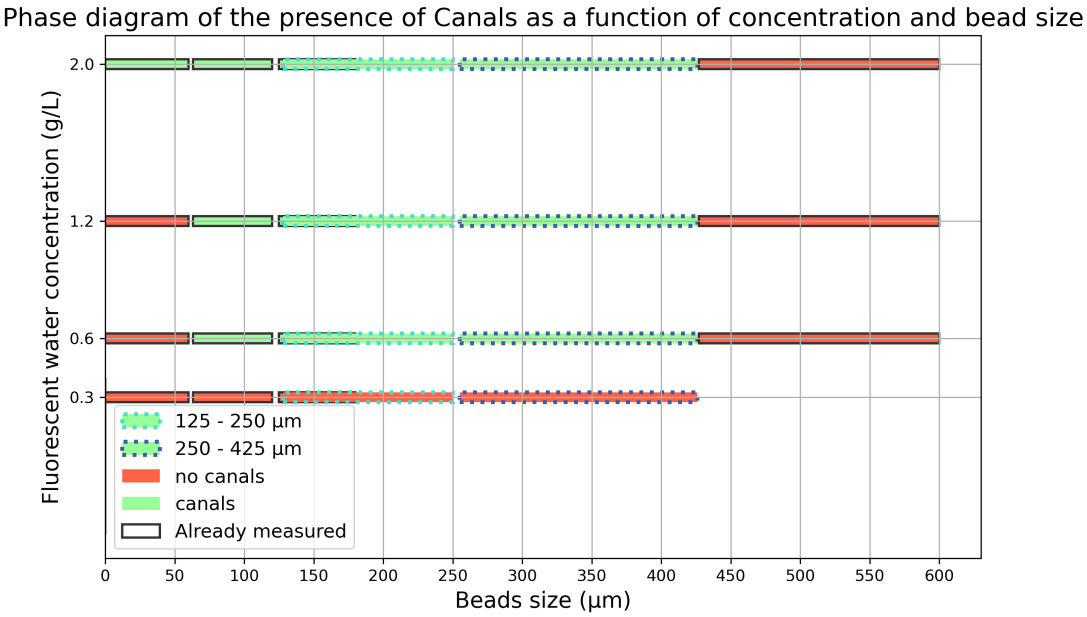

Figure 28: Phase diagram showing the results of my experiments (dotted lines) and those already carried out by the team (solid lines).

We can see on the phase diagram that there is a region where the parameters are favorising the appearance of canals. This zone covers ranges of size from $63\mu mto425\mu m$ for fluorecein concentration from $0.6g/Lto2g/L$. A further study of the dynamic of the fluxes between water grains and fluorecein would help to understand this phenomenon and see how relevant the mullins sekerka model is to our experience.

5 Freezing water with fluorecein

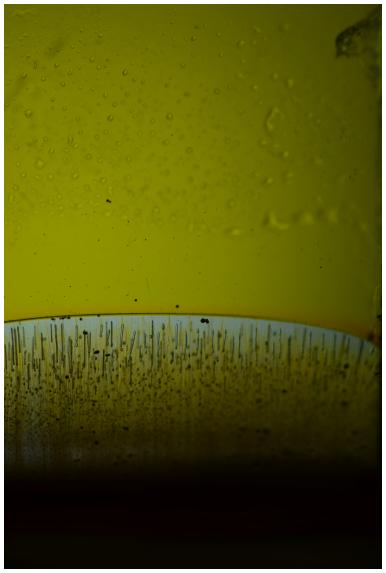

Figure 29: Pure water with fluo channels

Figure 30:

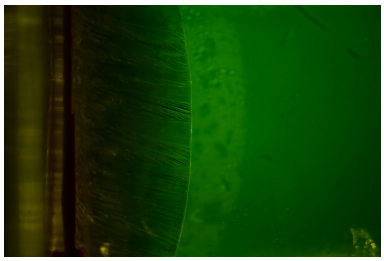

Figure 31:

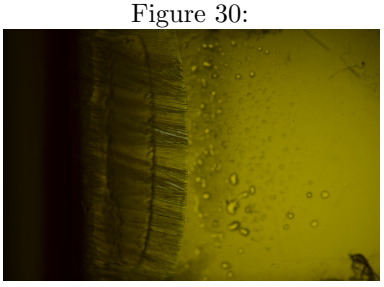

Figure 32:

Figure 33: channels

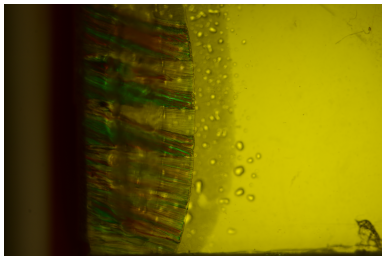

Figure 34:

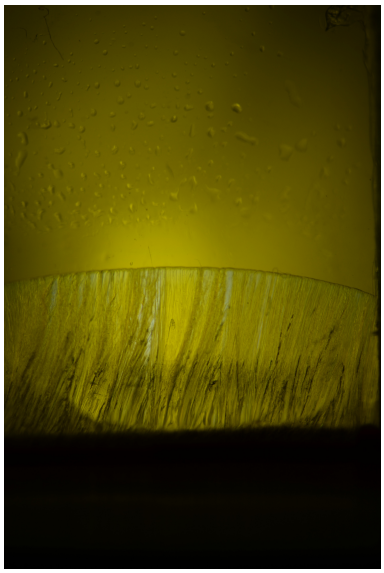

Figure 35:

6 Conclusion

In this course I studied the characteristics of a model soil subjected to solidification, which is comparable to the active layer associated with permafrost. My first area of interest was to characterise the dynamics of the solidification front and, more precisely, the growth as a function of time. I found that the front height of my model soil grows as a square root of time with an diffusif coefficient bigger than the one of water. The mix of water and grains due to the better diffusive caracteristics of the grains. Secondly, I focused on the study of the front instabilities pattern. I completed the phase diagram, started by my team, of the presence of channels in the solide phase with the 2 new ranges of grains size. An area stands out in the phase diagram where the parameters appear to be conducive for the creation of channels. For a further study, would be interesting for the first study of the front growth to find analytically the exact coefficient of the mix of water and grains and compare it with the experimental one. Concerning the second study about instabilities, we could look at the periodicity of the channel and relate it with the theoretical Mullins-Sekerka instabilities pattern wave length. Finally, this experience in the new IFADyFE laboratory not only strengthened my technical skills, but also my ability to solve problems independently and innovatively and discuss with the other labs to compensate for the lack of equipment in this laboratory in development.

7 Annexe

7.1 More on the experimental Setup

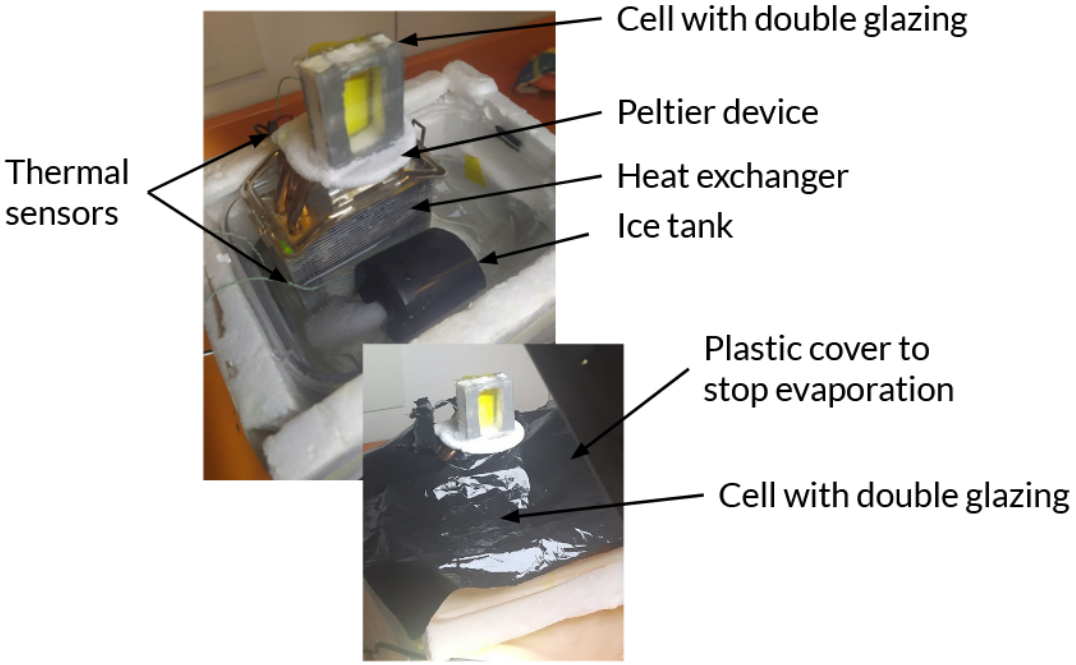

Figure 36: Photo of the experiment

Figure 37:

7.2 Solutions to condensation

The problem of condensation was at the heart of a large part of my work placement. To understand the context, the new ifadyfe premises are in blind rooms with no windows and far from all sources of outside air.

Ventilation is used to renew the air. What's more, the premises are not equipped with a column of dry air, which would have solved the problem more easily.

Below, I detail the different solutions I tested. For each of them, I had to find out how it worked, find a supplier to buy it and evaluate its effectiveness on several experimental manipulations.

Method	**Efficiency / Comments**
Spit and Soap	Works but requires regular manual applications
Aquarium with Silica gel and fans	Unable to prevent humid air from entering the aquarium; needed to regularly add new ice cubes by opening the aquarium
Spray dry air aerosol bomb	Convenient hand-held bomb with short-lived effects
Dry air with pump and filter	Technically challenging to implement
Dehumidifier	Similar to the aerosol bomb
Anti-condensation spray	Had no effect
Anti-condensation liquid	Condensation gathered into droplets that needed to be regularly absorbed with paper or a brush
Anti-condensation film	Similar to the anti-condensation liquid
New, more ventilated room	No noticeable change
Brush / absorbent paper	Tedious, moves the cell and impractical as one must be careful not to obstruct the camera which takes an image every 20 seconds
Covered tank	Effective
Fans	Not effective
Double-glazed cell	2 sizes were tested: 0.7cm (work well) and 1 cm (does not work)

Table 2: Methods to prevent condensation

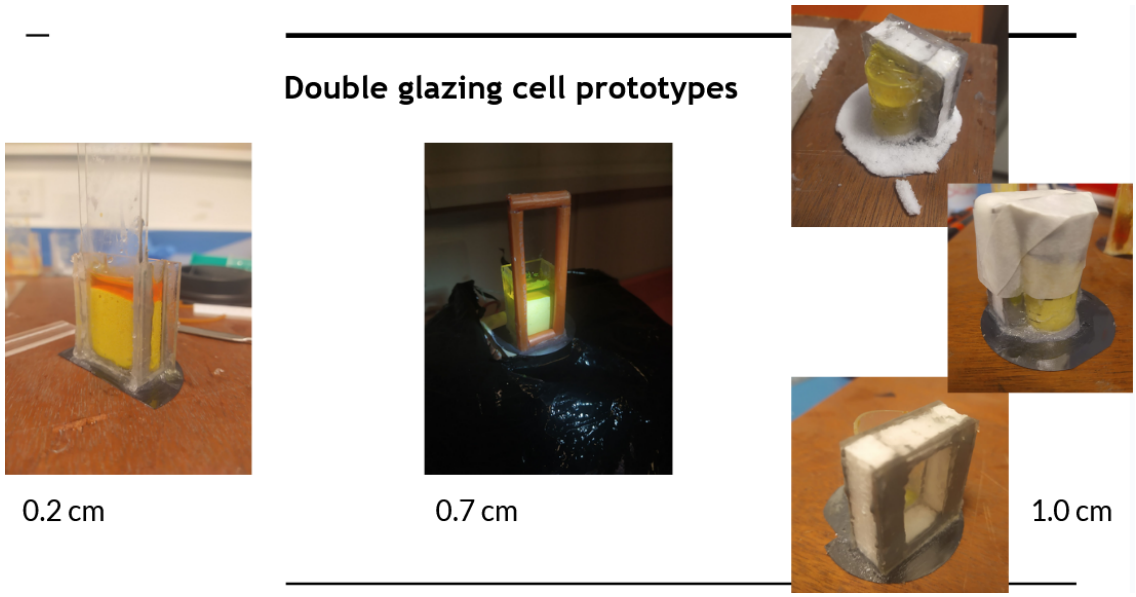

Figure 38: Some prototypes of double glazing cells

References

[1] *Base de données diffusivité thermique*. see values for Pyroceram 9606 ceramic glass and Pyroceram 9608 ceramic glass. URL: https://www.thermoconcept-sarl.com/base-de-donnees-diffusivite-thermique/.

[2] Krishan Bumma et al. "Early freezing dynamics of an aqueous foam". In: *Soft Matter* 19.28 (2023), pp. 5379–5384.

[3] Isabelle Cantat et al. "Directional solidification under stress". In: *Physical Review E* 58.5 (1998), p. 6027.

[4] Feng Cheng et al. "Alpine permafrost could account for a quarter of thawed carbon based on Plio-Pleistocene paleoclimate analogue". In: *Nature communications* 13.1 (2022), p. 1329.

[5] AOP Chiareli and M Grae Worster. "Flow focusing instability in a solidifying mushy layer". In: *Journal of Fluid Mechanics* 297 (1995), pp. 293–305.

[6] Francesc Font. "A one-phase Stefan problem with size-dependent thermal conductivity". In: *Applied Mathematical Modelling* 63 (2018), pp. 172–178. ISSN: 0307-904X. DOI: https://doi.org/10.1016/j.apm.2018.06.052. URL: https://www.sciencedirect.com/science/article/pii/S0307904X18303056.

[7] James S Langer. "Instabilities and pattern formation in crystal growth". In: *Reviews of modern physics* 52.1 (1980), p. 1.

[8] Anyuan Li et al. "Ice needles weave patterns of stones in freezing landscapes". In: *Proceedings of the National Academy of Sciences* 118.40 (2021), e2110670118.

[9] William W Mullins and RF Sekerka. "Stability of a planar interface during solidification of a dilute binary alloy". In: *Journal of applied physics* 35.2 (1964), pp. 444–451.

[10] Jaroslav Obu. "How much of the earth's surface is underlain by permafrost?" In: *Journal of Geophysical Research: Earth Surface* 126.5 (2021), e2021JF006123.

[11] Rubinshteı. *The stefan problem*. Vol. 27. American Mathematical Soc., 1971.

[12] Lila Seguy, Suzie Protiere, and Axel Huerre. "Role of geometry and adhesion in droplet freezing dynamics". In: *Physical Review Fluids* 8.3 (2023), p. 033601.

[13] Thomas Séon. “Hydrodynamique, Capillarité Changement de Phase”. In: *HDR* 5 (2021), p. 47.

[14] Virgile Thiévenaz, Thomas Séon, and Christophe Josserand. “Solidification dynamics of an impacted drop”. In: *Journal of Fluid Mechanics* 874 (2019), pp. 756–773.

[15] M Grae Worster and David W Rees Jones. “Sea-ice thermodynamics and brine drainage”. In: *Philosophical Transactions of the Royal Society A: Mathematical, Physical and Engineering Sciences* 373.2045 (2015), p. 20140166.